Study of Pd/MgO Catalysts for Furfural Alcohol Amination

Leela Prasad Y[1], Swamy Sekhar K[1], Venkateswara Rao B[1*], Raveendra Gundeboyina[2], Vijaya M[1], Hari Sekhar Mitta[3*]

[1]Department of Engineering Chemistry, Andhra University, Visakhapatnam-530003, India.

[2]Department of Process and Plant Engineering, Brandenburg University of Technology Cottbus–Senftenberg, Germany, 03046

[3]Laboratory for Chemical Technology (LCT), Department of Materials, Textiles and Chemical Engineering, Technology 125, 9052 Ghent, Belgium.

[*]Corresponding Author

DOI: https://dx.doi.org/10.47772/IJRISS.2024.8080278

Received: 13 August 2024; Accepted: 21 August 2024; Published: 19 September 2024

ABSTRACT

Recent interest in catalytic approaches has focused on their efficiency in converting biomass into chemicals and fuels. Palladium-based catalysts, in particular, are highly valued in industry. This study systematically evaluates the structural and catalytic properties of palladium catalysts supported on MgO with varying Pd loadings. Catalysts with Pd loadings ranging from 0.5 to 6 wt% were prepared using palladium chloride as a precursor. Characterization techniques including XRD, BET surface area analysis, XPS, UV-DRS, TPR, TPD of CO_2, and CO chemisorption were employed. Results showed that CO uptake, palladium metal surface area, and Pd density increased with Pd loading up to 2 wt% and then decreased with higher loadings. Furfural reductive amination over palladium supported on MgO catalysts showed an increase in furfuryl amine production with higher Pd loading. The relationship between palladium dispersion and furfural reductive amination activity was investigated.

Keywords: Pd, MgO, Furfural, Hydrogenation, Amination

INTRODUCTION

In recent times, due to the limited availability of fossil resources and growing environmental concerns, the utilization of biomass for fuel and chemical production has gained significant attention (Besson, Gallezot, & Pinel, 2014; Chheda, Huber, & Dumesic, 2007; Deng, Zhang, & Wang, 2014; Ragauskas et al., 2006). Catalytic methods are particularly promising as they can efficiently convert biomass into various liquid fuels and chemicals (Liu & Zhang, 2016). As a result, significant efforts have been focused on developing and applying different catalysts for biomass conversion. Palladium-based catalysts play a crucial role in various industrial reactions, such as DeNOx (Barbaro, Liguori, & Moreno-Marrodan, 2016; Jen et al., 1999; Roylance, Kim, & Choi, 2016), methanol decomposition (Sun, Lu, Wang, & Xu, 2004), methane steam reforming (Ozkan, Kumthekar, & Karakas, 1998), NO reduction with hydrocarbons(Bekyarova, Fornasiero, Kašpar, & Graziani, 1998), and CO hydrogenation (Shen, Okumura, Matsumura, & Haruta, 2001). The performance of these catalysts depends on the exposed percentage or dispersion of the active component on the support surface.

Oxygen-containing compounds are currently of interest due to their low cost and minimal use of reducing

agents during chemical conversion processes (Kobayashi, Ohta, & Fukuoka, 2012; Rinaldi & Schüth, 2009; Ruppert, Weinberg, & Palkovits, 2012). Furfuryl alcohol, used in the production of ascorbic acid, lysine, and lubricants, is a priority target (Nagaraja et al., 2003). Commercially, furfuryl alcohol is produced by selectively hydrogenating furfural using Cr-supported copper catalyst systems at high temperatures and pressures (Nagaraja, Padmasri, Raju, & Rao, 2007; Nakagawa, Tamura, & Tomishige, 2013). However, this method has limitations, including environmental pollution from toxic chromium in the catalyst and high energy costs. Therefore, the development of efficient Cr-free catalysts with improved activity, selectivity, recyclability, and performance under relevant reaction conditions is a key focus (Taylor et al., 2016). In recent years, various Cr-free catalyst systems, such as Pd, Pt, Rh, Ru, Au, and Ir, have shown enhanced catalytic activity for furfural hydrogenation under mild conditions. Different metal-supported and non-supported metal heterogeneous catalyst systems on Fe, Co, Ni, and Cu have been explored, but they have limitations in terms of activity, reaction temperatures, and selectivity. To improve conversion and selectivity, doping with appropriate hetero atoms has been investigated (Fulajtárova et al., 2015; Gong et al., 2017; Kotbagi, Gurav, Nagpure, Chilukuri, & Bakker, 2016; Srivastava et al., 2015; Tamura, Tokonami, Nakagawa, & Tomishige, 2013; Wu et al., 2017; Xiong, Wan, & Chen, 2016). Magnesium oxide is a suitable model oxide due to its simple structure and surface defects chemistry. Magnesia-supported catalysts have shown high catalytic potential in furfural hydrogenation.

Various Mg-based catalyst systems such as Mg/Cu-ZnO(Kong et al., 2017) Pt/Al_2O_3 supported Mg(Escobar, Barrera, Santes, & Terrazas, 2017), Ni/SiO_2/Mg(Ramesh et al., 2019), Mg/Co/Ni (Ding et al., 2020), Mg/TiO_2 (Meenashisundaram, Nai, Almajid, & Gupta, 2015), Mg/ZnO(Etacheri, Roshan, & Kumar, 2012) and Mg-doped graphene oxide/WS_2/ZnO (C. Chen, Yu, Liu, Cao, & Tsang, 2017) have been studied for hydrogenation and other reactions, showing promising results. This study focuses on investigating the structural and catalytic properties of palladium catalysts supported on MgO with varying Pd loading. Various spectroscopic and adsorption methods were used for catalyst characterization, analyzing palladium dispersion, and metal-support interactions. The catalytic properties were evaluated for the hydrogenation and reductive amination of furfural to cyclohexanone and aniline, correlating the results with palladium dispersion and other characterization techniques.

EXPERIMENTAL SECTION

Chemicals and materials

The reagents used in this study were purchased from Aldrich chemicals suppliers and SRL, Mumbai, India. They include Tetra-ethyl ortho-silicate (TEOS, 98%—from Aldrich), Cetyl trimethyl-ammonium bromide (CTAB from Aldrich), NaOH (80% from SRL, India), $Cu(NO_3)_2.6H_2O$ (98% from Aldrich), and NH_3 solution (30%, from SRL, India).

Catalyst Synthesis

MgO–supported palladium catalyst preparation

Palladium catalysts supported on MgO with different Pd loadings (0.5, 1, 2, 4, and 6 wt%) were prepared using a wet impregnation method. The MgO support had a BET surface area of 48 m2/g. The impregnated samples were dried at 383 K for 12 hours and then calcined in air at 773 K for 5 hours. The palladium chloride from Aldrich was used as the precursor in an acidic solution for impregnation.

Characterization

The catalysts underwent characterization using a range of spectroscopic and adsorption techniques including XRD, BET surface area analysis, pore size distribution measurement, UV-DRS analysis, XPS analysis,

TPR, TPD of CO_2, and CO chemisorption methods. The catalytic performance was evaluated in the hydrogenation of furfural to cyclohexanone and the reductive amination of furfural to aniline.

RESULTS AND DISCUSSION

X-ray diffraction (XRD)

The X-ray diffraction results of pure MgO and various Pd/MgO catalysts are shown in Figure 1. All samples display strong reflections at 2θ = 42.3°, 61.5°, and 77.3°, corresponding to the (200), (220), and(311) crystal planes of the MgO support. The XRD patterns exhibit sharp peaks without any additional peaks, indicating the absence of significant PdO characteristic peaks in the XRD spectra of 1wt% Pd/MgO and 2wt% Pd/MgO. This suggests that palladium oxide species are present in a highly dispersed amorphous state at lower Pd loadings. At Pd concentrations below 2 wt%, the palladium species are finely dispersed on the MgO matrix. However, at higher Pd loadings (> 2 wt% of Pd), XRD reflections from the PdO phase are observed at 2θ = 33.9°, 41.9°, and 54.4°, indicating an increase in the crystallinity of PdO with higher Pd loading. Previous studies have shown that no new peaks appear with Fe loading below 3 wt% on Fe/MgO catalysts, likely due to solid solution formation between Fe3+ and MgO support (C. Chen et al., 2017; Lin et al., 2004). Similarly, no crystalline NiO phase was observed up to 35 mol% loading on MgO support, attributed to solid-solution formation. In contrast, no solid solution formation was detected between PdO and MgO in palladium-supported MgO catalysts, as evidenced by the absence of crystalline PdO peaks even at 6 wt% loading (Hu & Ruckenstein, 1996). These results suggest an amorphous nature of the palladium species on the MgO support., with XRD patterns confirming the absence of characteristic peaks indicating mixed oxide phase formation between PdO and MgO support.

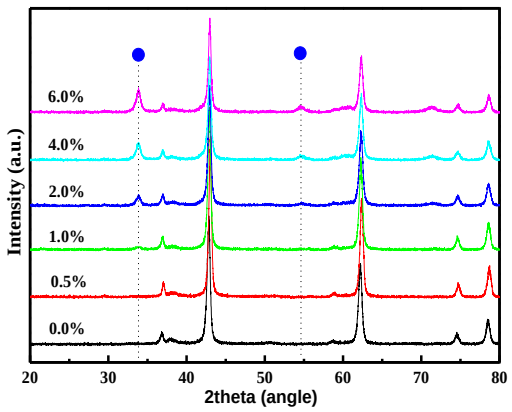

Figure 1: X-ray diffraction patterns of pure MgO and various Pd/MgO catalysts

BET surface area & Pore size distribution measurements

Table 1 presents the specific surface areas of different Pd/MgO catalysts as determined through nitrogen physisorption. The BET surface area of pure MgO was measured at 48 m2/g. As the Pd content on the MgO support increased, the specific surface area decreased. This decrease may be due to the blockage of support pores by palladium oxide crystallites, as indicated by XRD and pore size distribution analyses. Pore size distribution measurements were conducted on pure MgO and different Pd/MgO catalysts using a mercury intrusion porosimeter, assuming the presence of open-ended cylindrical pores. Table 1 provides details on the average pore diameter, total pore area, and total pore volume of the various Pd/MgO catalysts. It was observed that the total pore diameter, pore area, and pore volume decreased as the palladium loading increased. This decrease could be attributed to pore blockage by the palladium and the physical deposition of palladium oxide on the support surface.

ISSN No. 2454-6186 | DOI: 10.47772/IJRISS |Volume VIII Issue VIII August 2024

Table 3 Results of BET surface area and pore size distribution measurements for various Pd/MgO catalysts

Pd loading (wt.%)	BET surface area (m2/g)	Total pore volume (mL/g)	Total pore area (m2/g)	Average pore diameter (Å)
0.0	48	3.87	90	256
0.5	45	2.13	92	176
1.0	40	—	—	—
2.0	35	1.95	87	157
4.0	33	—	—	—
6.0	29	1.56	87	139

CO chemisorption

Table 2 shows the Pd dispersion, crystallite size, and metal area obtained from irreversible CO chemisorption on Pd supported on MgO catalysts calcined at 773 K Pd dispersion ranged from 13.2% to 3.0%, with higher dispersion at lower Pd concentrations due to strong interaction with the support. Pd dispersion and metal area decrease with increasing Pd loading. Crystallite size increases with Pd loading, indicating agglomeration of larger crystallites. XRD results support this observation. CO uptake and metal area increase up to 2 wt.% Pd loading, then plateau. Figure 2 shows a correlation between these properties and Pd loadings, with CO uptake, Pd metal surface area, and Pd density increasing up to 2 wt.% Pd loading and then stabilizing. Metal surface area and CO uptake remain constant at higher Pd loadings due to the depletion of active sites.

Table 4 Results of CO uptake, dispersion, metal area, and average particle size of various Pd/MgO catalysts

Pd loading (wt.%)	Dispersion (%)	CO_{irr} uptake ($\mu mol/g_{cat}$)	Metal area (m^2/g_{pd})	Metal area (m^2/g_{cat})	Crystallite size (nm)
0.5	13.2	6.2	58.7	0.29	8.5
1.0	9.7	9.2	43.4	0.43	11.5
2.0	7.6	14.4	34.0	0.67	19.7
4.0	4.4	16.6	19.7	0.78	25.4
6.0	3.0	17.0	13.4	0.80	37.2

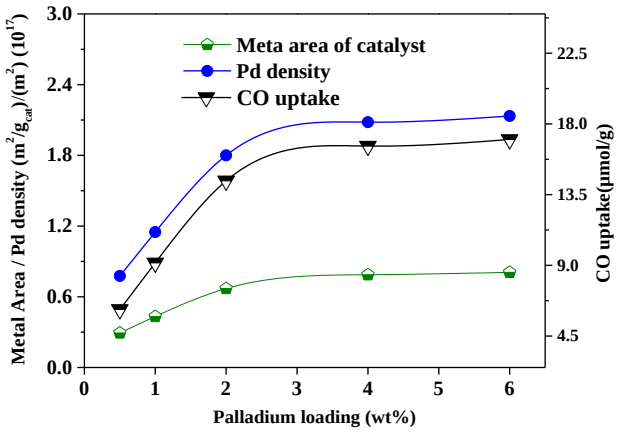

Figure 2: Effect of metal loading on metal surface area, Pd density, and CO uptake of Pd supported on MgO catalysts

ISSN No. 2454-6186 | DOI: 10.47772/IJRISS |Volume VIII Issue VIII August 2024

UV-Vis diffuse reflectance spectroscopy

The nature of palladium active species on Pd/MgO can be determined using the UV-DRS technique, which reveals information about the coordination of palladium in the clusters (Aytam et al., 2002; Boukha, Kacimi, Ziyad, Ensuque, & Bozon-Verduraz, 2007; Ferreira, De Oliveira, & Noronha, 2004; Hu & Ruckenstein, 1996). UV-Vis DRS spectroscopy helps estimate changes in the coordination geometry and ligands of surface palladium oxide cations on various supports, as well as detect changes in the domain size of dispersed palladium. The UV-DR spectra of loaded Pd/MgO samples show two strong adsorption bands at 260 nm and 510 nm, indicating ligand metal charge transfer and d-d transitions of Pd^{2+} ions, respectively. The LMCT absorption at 260 nm increases with Pd loading, suggesting more Pd^{2+} ions linked with surface oxygen atoms. The d-d transition band at 510 nm shifts to higher wavelengths with increased Pd loading, indicating interfacial charge transfer between Pd^{2+} and MgO. The intensity of the absorption band at 510 nm increases with higher Pd loadings, suggesting the presence of crystallites or bulk PdO. At lower loadings, there is no indication of LMCT or d-d transitions, possibly due to the dilution of Pd^{2+} ions in the MgO matrix. The UV-DRS results indicate the presence of dispersed palladium and bulk PdO in Pd/MgO, consistent with XRD results showing increased intensities of PdO reflections with higher Pd loading.

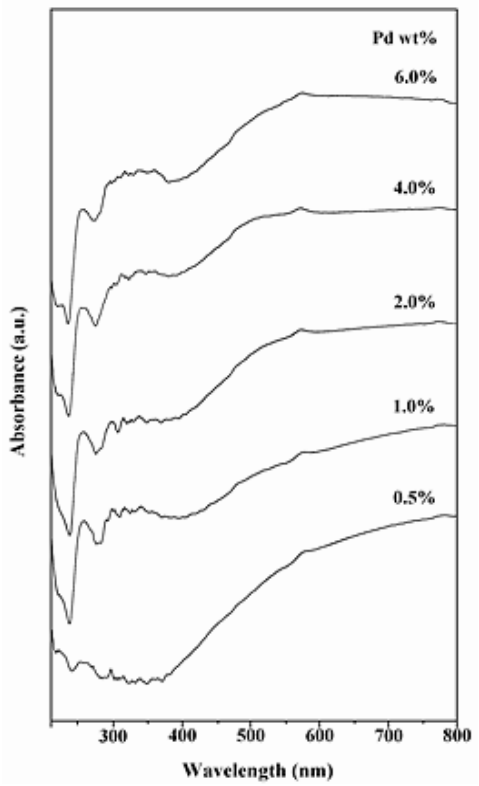

Figure 3: UV-Vis diffuse reflectance spectra of different Pd/MgO catalysts

X-ray photoelectron spectroscopy

The surface palladium species of Pd/MgO catalysts were analyzed using XPS (table 3). The Mg 2p3/2 binding energy values were around 49.9± 0.2 eV. The intensities of Mg 2p core-level spectra did not change with increasing palladium loading(Fleisch, Hicks, & Bell, 1984; Lederhos, L'Argentière, & Fígoli, 2005; Takasu, Unwin, Tesche, Bradshaw, & Grunze, 1978; Voogt, Mens, Gijzeman, & Geus, 1999), results are presented in Table 3. XPS results for Pd 3d5/2 and Pd 3d3/2 on MgO-supported palladium catalysts showed binding energy values between 336.7-336.9 eV and 342.2-342.5 eV results are consistent with CO chemisorption, UV-DRS, and other techniques used to determine palladium dispersion on the support.

ISSN No. 2454-6186 | DOI: 10.47772/IJRISS |Volume VIII Issue VIII August 2024

Table 3: Binding energies (eV), FWHM, XPS atomic ratios of Pd 3d5/2 and Mg 2p for Pd/MgO catalysts

Pd loading (wt%)	Position and FWHM of Mg 2p3/2	Position and FWHM of Pd 3d5/2	XPS intensity Pd 3d/Mg 2p
0.5	49.9 (2.2)	336.9 (2.3)	0.046
1.0	49.8 (2.1)	336.8 (2.3)	0.081
2.0	50.0 (2.2)	336.7 (2.4)	0.11
4.0	50.1 (2.2)	336.7 (2.4)	0.10

Temperature programmed reduction

Figure 4 displays the temperature-programmed reduction profiles of palladium supported on MgO catalysts. Three distinct peaks were observed in the reduction temperature ranges of 365-401 K, 447-465 K, and 621-653 K. The peaks at 365-401 K corresponded to the reduction of dispersed Pd2+ species and bulk PdO, while the peak at 447-465 K was attributed to hydrogen spillover from metallic Pd to the MgO support(Y. Chen, Hwang, & Liaw, 1998; ITO, 1987). The higher temperature peak at 621-653 K indicated the reduction of the MgO support(Pillai & Sahle-Demessie, 2004; Tichit et al., 2007). The maximum reduction temperature (Tmax) decreased from 401 K for 0.5 wt% Pd to 365 K for 2 wt% Pd, indicating highly dispersed Pd particles at lower loadings and a strong metal-support interaction. The intensity of the low-temperature peak in TPR increased with additional palladium loading, while the intensity of the high-temperature peaks decreased. This suggests that a strong metal-support interaction enhances spillover and facilitates support reduction at lower loadings. The TPR profiles and H_2 uptake were proportional to the Pd loading, with no characteristic negative peak of β-PdHx observed in the TPR of Pd/MgO catalysts. Quantitative data on hydrogen consumption and Tmax positions against Pd loading are provided in Table 4.

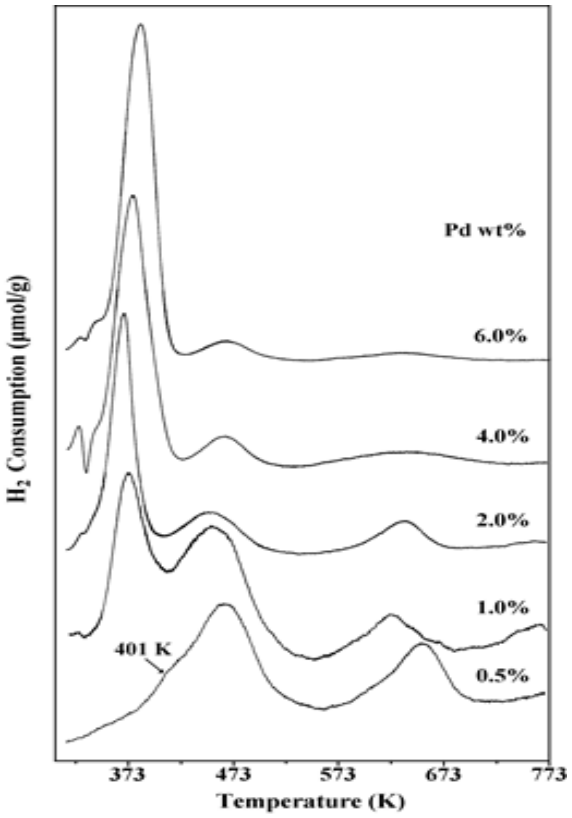

Figure 4: Temperature-programmed reduction profiles of various Pd/MgO catalysts

ISSN No. 2454-6186 | DOI: 10.47772/IJRISS |Volume VIII Issue VIII August 2024

Table 4: Temperature programmed reduction results of various Pd/MgO Catalysts

Pd loading (wt%)	T_{max}^1 (K)	H_2 Consumption (µmol/g)	T_{max}^2 (K)	H_2 Consumption (µmol/g)	T_{max}^3 (K)	H_2 Consumption (µmol/g)
0.5	401.3	38.63	464.4	151.95	652.9	123.13
1.0	372.2	69.88	450.6	84.43	621.3	62.21
2.0	365.5	220.75	447.5	69.81	635.9	30.13
4.0	372.5	334.57	461.8	34.12	636.1	15.62
6.0	379.5	731.39	463.7	38.19	636.0	9.46

Temperature-programmed desorption of CO_2

Solid catalysts with acidic and basic sites on their surface play a crucial role in catalysis. The acid-base properties of the support affect catalytic activity by interacting with active components or providing bifunctional sites (Pérez-Zurita et al., 2003). Studies on palladium catalysts supported on layered double hydroxides and MgO have shown the importance of acid-base properties in catalytic reactions(Aramendıa et al., 2004; Scire, Crisafulli, Maggiore, Minicò, & Galvagno, 1998). Temperature-programmed desorption (TPD) of strong basic sites based on TPD profiles. The basicity of Pd/MgO catalysts increases with palladium loading up to 2 wt% and then decreases, indicating the role of well-dispersed palladium sites(Claus et al., 2000; Corma, Ródenas, & Sabater, 2010; Escobar et al., 2017; Kong et al., 2017; Luo, Pu, He, Jin, & Jin, 2006; Pothu et al.; Pothu et al., 2023; Tichit, Coq, Cerneaux, & Durand, 2002). The decline in basicity at higher palladium loadings may be due to palladium agglomeration. The basicity of the catalysts influences their activity in hydrogenation and reductive amination reactions. The basicity is mainly attributed to the palladium phase, as indicated by CO_2 uptake and CO chemisorption measurements (Table 5)

Table 5: Temperature-programmed CO_2-desorption of pure MgO and various Pd/MgO catalysts

Pd loading (wt%)	CO_2 uptake (µmol/g)			Total basicity (µmol/g)
	Weak	Medium	Strong	
0.0	—	3404	—	3404
0.5	32	199	—	231
2.0	37	222	27	286
4.0	30	198	35	263
6.0	28	193	33	254

Hydrogenation of furfural

The vapor phase hydrogenation of furfural-to-furfural alcohol at 453 K over various Pd/MgO catalysts is shown in Figure 5a. Furfural conversion and product selectivity depend on Pd loading and support nature. Furfural conversion increases with Pd loading up to 2 wt.% and levels off thereafter due to enhanced palladium crystallinity (figure 2). This trend correlates with CO chemisorption and the metal area of the catalyst. Basic strength increases up to 2 wt.% Pd loading and decreases at higher loadings, affecting furfural conversion and selectivity. Furfuryl alcohol selectivity is 95% for 0.5 wt.% Pd decreases to 90% for 2 wt.% Pd and remains stable at higher loadings. Furfural molecules adsorb on the oxide surface near Pd active sites and react with hydrogen atoms on Pd crystallites. Furfural is first

ISSN No. 2454-6186 | DOI: 10.47772/IJRISS |Volume VIII Issue VIII August 2024

hydrogenated to furfural alcohol, with rapid hydrogenation near the acidic support. Increased basicity up to 2 wt.% Pd promotes furfural alcohol formation. XPS, CO chemisorption and basic properties support the catalytic properties of Pd/MgO catalysts. TOF vs Pd loading (Figure 5b) shows a structure-activity relationship in furfural hydrogenation. TOF decreases with Pd loading up to 2 wt.% and is less significant at higher loadings. Per-site activity is highest by 0.5 wt.% Pd and decreases with more Pd loading. Structural sensitivity of furfural hydrogenation is observed over Pd/MgO catalysts, with TOF varying with Pd loading and crystallite size. High activity at low Pd content (up to 2 wt.%) is due to Pd dispersion over MgO support, while activity decreases with higher Pd loading due to increased Pd crystallinity. This indicates that furfural hydrogenation over Pd/MgO catalysts is structure-sensitive (Scheme 1).

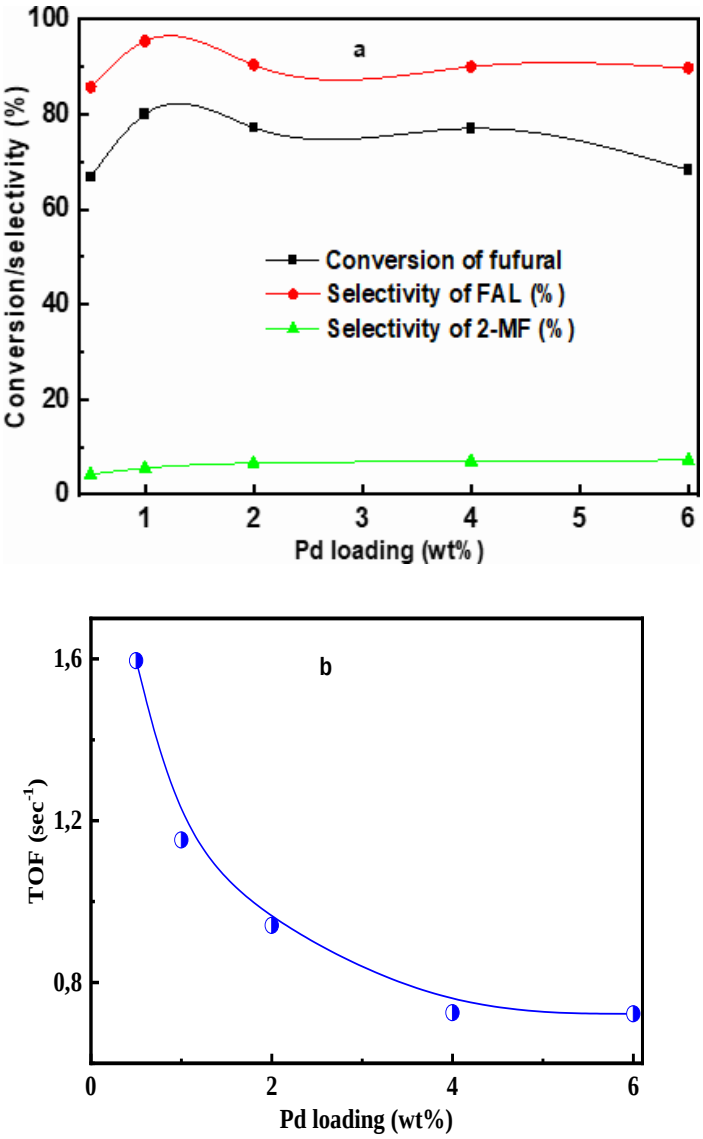

Figure 5: (a) Hydrogenation of Furfural over various Pd/MgO catalysts; (b) Relation between TOF Vs palladium loading

Reductive amination of furfural to furfuryl amine

Reductive amination of furfural to furfuryl amine. The catalytic properties of Pd supported on MgO were studied for the vapor-phase reductive amination of furfural to furfuryl amine. The presence of Pd δ+ species promotes the interaction of furfural and ammonia, leading to the formation of furfuryldemine. Subsequent hydrogenation of furfuryldemine with H_2 results in the production of furfuryl amine. The use of

ISSN No. 2454-6186 | DOI: 10.47772/IJRISS |Volume VIII Issue VIII August 2024

precious metals like Pd in this reaction offers advantages due to their superior hydrogenation capabilities. Tautomerization of furfuryldemine occurs on acidic supports, facilitating the desorption of the intermediate and the formation of furfuryl amine. The hydrogenation of furfural to furfuryldemine is the rate-limiting step in the reductive amination process. Furfural alcohol reacts with ammonia to form furfuryldemine, which is then hydrogenated in the presence of palladium to yield furfuryl amine. The Pd/MgO catalyst contains Pd metallic active sites for hydrogenation and dehydrogenation reactions, as well as weak acidic sites for isomerization and amination reactions.

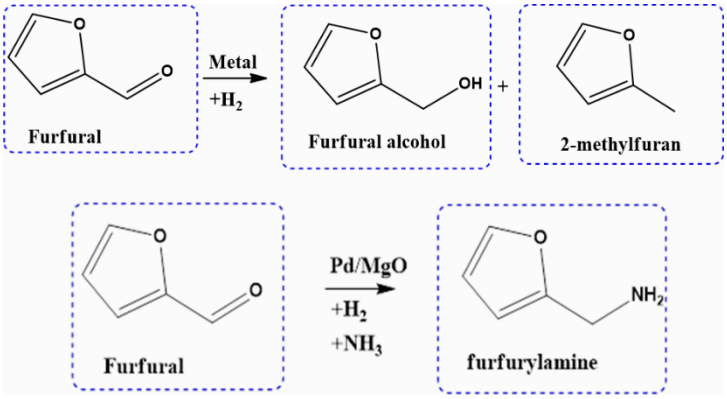

Scheme 1: Reaction of furfural to furfuryl amine in the presence of Pd/MgO catalyst

In this study on the reductive amination of Furfural using palladium supported on MgO catalysts, furfurylamine ($C_4H_3OCH_2$-NH_2) was identified as the main product (Figure 6). The conversion of Furfural increased with up to 2 wt.% Pd loading then decreased at higher loadings. This trend correlates with the amount of CO-chemisorbed and the metal area of the catalyst (Figure 2). The strength of basic sites also increased with Pd loading up to 2 wt.%, indicating a direct relationship between Furfural conversion, active Pd sites, and the basic strength of the catalyst. Selectivity towards aniline formation decreased with increasing Pd loading up to 2 wt.% and remained constant at higher loadings. The relationship between Furfural reductive amination and palladium loading is illustrated in Figure 10, showing the structure-activity relationship between palladium dispersion and activity. The turnover frequency (TOF) decreased with increasing Pd loading up to 2 wt.% and became less significant beyond this point. Changes in per-site activity (TOF) were observed concerning crystallite size, highlighting the structure-sensitive nature of the reaction over palladium supported on MgO. The decrease in TOF with increasing Pd loading may be attributed to the decline in Pd dispersion on the MgO support. These catalytic results align well with Pd dispersion data and information obtained from other techniques.

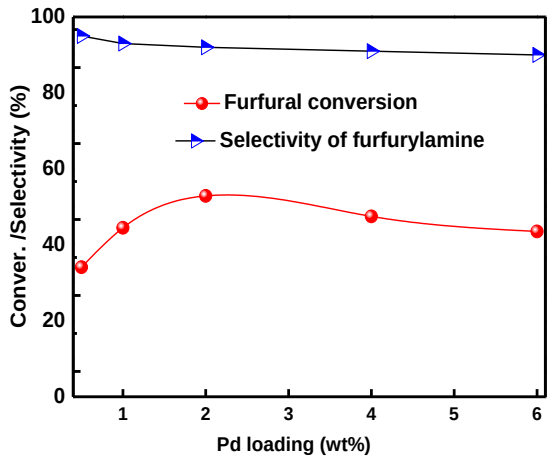

Figure 6: Reductive amination of Furfural over different Pd/MgO catalysts

CONCLUSION

In this study, we investigated the structural and catalytic properties of palladium catalysts supported on MgO with varying Pd loading. CO chemisorption studies revealed a correlation between CO uptake, palladium metal surface area, and Pd density, increasing up to 2 wt.% Pd loading and decreasing at higher loadings. CO_2 uptake studies supported these results. The total basicity of the catalysts increased with Pd loading up to 2 wt.% and then decreased. Furfural conversion and catalyst basicity showed a similar trend. The constant conversion of catalysts beyond 2 wt.% Pd loading was attributed to increased palladium crystallinity. Furfuryl amine conversion rate increased with higher Pd loading due to CO chemisorption and metal area. The relationship between palladium dispersion and Furfural reductive amination activity showed a decline in turnover frequency (TOF) up to 2 wt.% Pd loading. These findings were consistent with Pd dispersion results and data from other techniques.

ACKNOWLEDGMENTS

One of the authors, Leela Prasad, thanks to Andhra University management. We acknowledge HM, SSK, RG, and HM. Statements made herein are solely the responsibility of the authors.

DECLARATION OF COMPETING INTEREST

The authors declare no conflict of interest.

REFERENCES

1. Aramendıa, M. A., Borau, V., Jiménez, C., Marinas, A., Marinas, J. M., Ruiz, J. R., et al. (2004). Magnesium-containing mixed oxides as basic catalysts: base characterization by carbon dioxide TPD–MS and test reactions. *Journal of Molecular Catalysis A: Chemical, 218*(1), 81-90.
2. Aytam, H. P., Akula, V., Janmanchi, K., Kamaraju, S. R. R., Panja, K. R., Gurram, K., et al. (2002). Characterization and reactivity of Pd/MgO and Pd/ γ-Al2O3 catalysts in the selective hydrogenolysis of CCl2F2. *The Journal of Physical Chemistry B, 106*(5), 1024-1031.
3. Barbaro, P., Liguori, F., & Moreno-Marrodan, C. (2016). Selective direct conversion of C 5 and C 6 sugars to high added-value chemicals by a bifunctional, single catalytic body. *Green Chemistry, 18* (10), 2935-2940.
4. Bekyarova, E., Fornasiero, P., Kašpar, J., & Graziani, M. (1998). CO oxidation on Pd/CeO2–ZrO2 catalysts. *Catalysis Today, 45*(1-4), 179-183.
5. Besson, M., Gallezot, P., & Pinel, C. (2014). Conversion of biomass into chemicals over metal catalysts. *Chemical reviews, 114*(3), 1827-1870.
6. Boukha, Z., Kacimi, M., Ziyad, M., Ensuque, A., & Bozon-Verduraz, F. (2007). Comparative study of catalytic activity of Pd loaded hydroxyapatite and fluoroapatite in butan-2-ol conversion and methane oxidation. *Journal of Molecular Catalysis A: Chemical, 270*(1-2), 205-213.
7. Chen, C., Yu, W., Liu, T., Cao, S., & Tsang, Y. (2017). Graphene oxide/WS2/Mg-doped ZnO nanocomposites for solar-light catalytic and anti-bacterial applications. *Solar Energy Materials and Solar Cells, 160*, 43-53.
8. Chen, Y., Hwang, C., & Liaw, C. (1998). One-step synthesis of methyl isobutyl ketone from acetone with calcined Mg/Al hydrotalcite-supported palladium or nickel catalysts. *Applied Catalysis A: General, 169*(2), 207-214.
9. Chheda, J. N., Huber, G. W., & Dumesic, J. A. (2007). Liquid-phase catalytic processing of biomass-derived oxygenated hydrocarbons to fuels and chemicals. *Angewandte Chemie International Edition, 46*(38), 7164-7183.

10. Claus, P., Berndt, H., Mohr, C., Radnik, J., Shin, E.-J., & Keane, M. A. (2000). Pd/MgO: catalyst characterization and phenol hydrogenation activity. *Journal of Catalysis, 192*(1), 88-97.
11. Corma, A., Ródenas, T., & Sabater, M. J. (2010). A Bifunctional Pd/MgO Solid Catalyst for the One-Pot Selective N-Monoalkylation of Amines with Alcohols. *Chemistry–A European Journal, 16* (1), 254-260.
12. Deng, W., Zhang, Q., & Wang, Y. (2014). Catalytic transformations of cellulose and cellulose-derived carbohydrates into organic acids. *Catalysis Today, 234*, 31-41.
13. Ding, X., Ding, H., Song, Y., Xiang, C., Li, Y., & Zhang, Q. (2020). Activity-tuning of supported co–ni nanocatalysts via composition and morphology for hydrogen storage in MgH2. *Frontiers in Chemistry*, *7*, 937.
14. Escobar, J., Barrera, M. C., Santes, V., & Terrazas, J. E. (2017). Naphthalene hydrogenation over Mg-doped Pt/Al2O3. *Catalysis Today*, *296*, 197-204.
15. Etacheri, V., Roshan, R., & Kumar, V. (2012). Mg-doped ZnO nanoparticles for efficient sunlight-driven photocatalysis. *ACS applied materials & interfaces, 4*(5), 2717-2725.
16. Ferreira, R., De Oliveira, P., & Noronha, F. (2004). Characterization and catalytic activity of Pd/V2O5/Al2O3 catalysts on benzene total oxidation. *Applied Catalysis B: Environmental, 50*(4), 243-249.
17. Fleisch, T. H., Hicks, R. F., & Bell, A. T. (1984). An XPS study of metal-support interactions on PdSiO2 and PdLa2O3. *Journal of Catalysis, 87*(2), 398-413.
18. Fulajtárova, K., Soták, T., Hronec, M., Vávra, I., Dobročka, E., & Omastová, M. (2015). Aqueous phase hydrogenation of furfural to furfuryl alcohol over Pd–Cu catalysts. *Applied Catalysis A: General*, *502*, 78-85.
19. Gong, W., Chen, C., Zhang, H., Zhang, Y., Zhang, Y., Wang, G., et al. (2017). Highly selective liquid-phase hydrogenation of furfural over N-doped carbon supported metallic nickel catalyst under mild conditions. *Molecular Catalysis, 429*, 51-59.
20. Hu, Y. H., & Ruckenstein, E. (1996). Temperature-programmed desorption of CO adsorbed on NiO/MgO. *Journal of Catalysis, 163*(2), 306-311.
21. ITO, T. (1987). Coordinative Unsaturation and Adsorptive and Catalytic Activities of Alkaline Earth Metal Oxides. *Hyomen Kagaku, 8*(6), 488-497.
22. Jen, H.-W., Graham, G., Chun, W., McCabe, R., Cuif, J.-P., Deutsch, S., et al. (1999). Characterization of model automotive exhaust catalysts: Pd on ceria and ceria–zirconia supports. *Catalysis Today, 50*(2), 309-328.
23. Kobayashi, H., Ohta, H., & Fukuoka, A. (2012). Conversion of lignocellulose into renewable chemicals by heterogeneous catalysis. *Catalysis Science & Technology, 2*(5), 869-883.
24. Kong, X., Chen, Z., Wu, Y., Wang, R., Chen, J., & Ding, L. (2017). Synthesis of Cu–Mg/ZnO catalysts and catalysis in dimethyl oxalate hydrogenation to ethylene glycol: enhanced catalytic behavior in the presence of a Mg 2+ dopant. *RSC advances, 7*(78), 49548-49561.
25. Kotbagi, T. V., Gurav, H. R., Nagpure, A. S., Chilukuri, S. V., & Bakker, M. G. (2016). Highly efficient nitrogen-doped hierarchically porous carbon supported Ni nanoparticles for the selective hydrogenation of furfural to furfuryl alcohol. *RSC advances, 6*(72), 67662-67668.
26. Lederhos, C. R., L'Argentière, P. C., & Fígoli, N. S. (2005). 1-heptyne selective hydrogenation over Pd supported catalysts. *Industrial & engineering chemistry research*, *44*(6), 1752-1756.
27. Lin, W., Zhu, Y., Wu, N., Xie, Y., Murwani, I., & Kemnitz, E. (2004). Total oxidation of methane at low temperature over Pd/TiO2/Al2O3: effects of the support and residual chlorine ions. *Applied Catalysis B: Environmental, 50*(1), 59-66.
28. Liu, B., & Zhang, Z. (2016). Catalytic conversion of biomass into chemicals and fuels over magnetic catalysts. *Acs Catalysis, 6*(1), 326-338.
29. Luo, M.-F., Pu, Z.-Y., He, M., Jin, J., & Jin, L.-Y. (2006). Characterization of PdO/Ce0. 8Y0. 2O1. 9 catalysts for carbon monoxide and methane oxidation. *Journal of Molecular Catalysis A: Chemical, 260*(1-2), 152-156.
30. Meenashisundaram, G. K., Nai, M. H., Almajid, A., & Gupta, M. (2015). Development of high

performance Mg–TiO2 nanocomposites targeting for biomedical/structural applications. *Materials & Design (1980-2015), 65*, 104-114.

31. Nagaraja, B., Kumar, V. S., Shasikala, V., Padmasri, A., Sreedhar, B., Raju, B. D., et al. (2003). A highly efficient Cu/MgO catalyst for vapour phase hydrogenation of furfural to furfuryl alcohol. *Catalysis communications, 4*(6), 287-293.
32. Nagaraja, B., Padmasri, A., Raju, B. D., & Rao, K. R. (2007). Vapor phase selective hydrogenation of furfural to furfuryl alcohol over Cu–MgO coprecipitated catalysts. *Journal of Molecular Catalysis A: Chemical, 265*(1-2), 90-97.
33. Nakagawa, Y., Tamura, M., & Tomishige, K. (2013). Catalytic reduction of biomass-derived furanic compounds with hydrogen. *ACS catalysis, 3*(12), 2655-2668.
34. Ozkan, U. S., Kumthekar, M. W., & Karakas, G. (1998). Characterization and temperature-programmed studies over Pd/TiO2 catalysts for NO reduction with methane. *Catalysis today, 40*(1), 3-14.
35. Pérez-Zurita, M. J., Cifarelli, M., Cubeiro, M. L., Alvarez, J., Goldwasser, M., Pietri, E., et al. (2003). Palladium-based catalysts for the synthesis of alcohols. *Journal of Molecular Catalysis A: Chemical, 206*(1-2), 339-351.
36. Pillai, U. R., & Sahle-Demessie, E. (2004). Selective oxidation of alcohols by molecular oxygen over a Pd/MgO catalyst in the absence of any additives. *Green chemistry, 6*(3), 161-165.
37. Pothu, R., Mameda, N., Boddula, R., Mitta, H., Perugopu, V., & Al-Qahtani, N. Materials Science for Energy Technologies.
38. Pothu, R., Mitta, H., Banerjee, P., Boddula, R., Srivastava, R. K., Kalambate, P. K., et al. (2023). Insights into the influence of Pd loading on CeO2 catalysts for CO2 hydrogenation to methanol. *Materials Science for Energy Technologies, 6*, 484-492.
39. Ragauskas, A. J., Williams, C. K., Davison, B. H., Britovsek, G., Cairney, J., Eckert, C. A., et al. (2006). The path forward for biofuels and biomaterials. *science, 311*(5760), 484-489.
40. Ramesh, A., Tamizhdurai, P., Mangesh, V., Palanichamy, K., Gopinath, S., Sureshkumar, K., et al. (2019). Mg/SiO2–Al2O3 supported nickel catalysts for the production of naphthenic hydrocarbon fuel by hydro-de-oxygenation of eugenol. *International Journal of Hydrogen Energy, 44*(47), 25607-25620.
41. Rinaldi, R., & Schüth, F. (2009). Design of solid catalysts for the conversion of biomass. *Energy & Environmental Science, 2*(6), 610-626.
42. Roylance, J. J., Kim, T. W., & Choi, K.-S. (2016). Efficient and selective electrochemical and photoelectrochemical reduction of 5-hydroxymethylfurfural to 2, 5-bis (hydroxymethyl) furan using water as the hydrogen source. *Acs Catalysis, 6*(3), 1840-1847.
43. Ruppert, A. M., Weinberg, K., & Palkovits, R. (2012). Hydrogenolysis goes bio: from carbohydrates and sugar alcohols to platform chemicals. *Angewandte Chemie International Edition, 51*(11), 2564-2601.
44. Scire, S., Crisafulli, C., Maggiore, R., Minicò, S., & Galvagno, S. (1998). Effect of the acid–base properties of Pd–Ca/Al2O3 catalysts on the selective hydrogenation of phenol to cyclohexanone: FT-IR and TPD characterization. *Applied surface science, 136*(4), 311-320.
45. Shen, W.-J., Okumura, M., Matsumura, Y., & Haruta, M. (2001). The influence of the support on the activity and selectivity of Pd in CO hydrogenation. *Applied Catalysis A: General, 213*(2), 225-232.
46. Srivastava, S., Mohanty, P., Parikh, J. K., Dalai, A. K., Amritphale, S., & Khare, A. K. (2015). Cr-free Co–Cu/SBA-15 catalysts for hydrogenation of biomass-derived α-, β-unsaturated aldehyde to alcohol. *Chinese Journal of Catalysis, 36*(7), 933-942.
47. Sun, K., Lu, W., Wang, M., & Xu, X. (2004). Characterization and catalytic performances of La doped Pd/CeO2 catalysts for methanol decomposition. *Applied Catalysis A: General, 268*(1-2), 107-113.
48. Takasu, Y., Unwin, R., Tesche, B., Bradshaw, A., & Grunze, M. (1978). Photoemission from palladium particle arrays on an amorphous silica substrate. *Surface Science, 77*(2), 219-232.
49. Tamura, M., Tokonami, K., Nakagawa, Y., & Tomishige, K. (2013). Rapid synthesis of unsaturated

alcohols under mild conditions by highly selective hydrogenation. *Chemical Communications, 49*(63), 7034-7036.

50. Taylor, M. J., Durndell, L. J., Isaacs, M. A., Parlett, C. M., Wilson, K., Lee, A. F., et al. (2016). Highly selective hydrogenation of furfural over supported Pt nanoparticles under mild conditions. *Applied Catalysis B: Environmental, 180*, 580-585.
51. Tichit, D., Coq, B., Cerneaux, S., & Durand, R. (2002). Condensation of aldehydes for environmentally friendly synthesis of 2-methyl-3-phenyl-propanal by heterogeneous catalysis. *Catalysis today, 75*(1-4), 197-202.
52. Tichit, D., Ortiz, M. d. J. M., Francová, D., Gérardin, C., Coq, B., Durand, R., et al. (2007). Design of nanostructured multifunctional Pd-based catalysts from layered double hydroxides precursors. *Applied Catalysis A: General, 318*, 170-177.
53. Voogt, E., Mens, A., Gijzeman, O., & Geus, J. (1999). XPS analysis of the oxidation of palladium model catalysts. *Catalysis today, 47*(1-4), 321-323.
54. Wu, J., Gao, G., Li, J., Sun, P., Long, X., & Li, F. (2017). Efficient and versatile CuNi alloy nanocatalysts for the highly selective hydrogenation of furfural. *Applied Catalysis B: Environmental, 203*, 227-236.
55. Xiong, K., Wan, W., & Chen, J. G. (2016). Reaction pathways of furfural, furfuryl alcohol and 2-methylfuran on Cu (111) and NiCu bimetallic surfaces. *Surface Science, 652*, 91-97.